Journal of Engineering Research and Applied Science
Available at www.journaleras.com
Volume 15 (1), June 2026, pp 98-106
ISSN 2147-3471 © 2026

Theoretical Study to Design Efficient Dye-Sensitized Solar Cell (DSSC): A DFT/TDDFT Approach

Hatice Vural*, Canan Oral

Electrical-Electronics Engineering, Amasya University, Amasya, Turkey

Accepted 22 June 2026

Abstract

The electronic and photovoltaic parameters of 2,2′-biquinoline-4,4′-dicarboxylic acid (2BA) were investigated using the B3LYP and M06-2X hybrid functionals of density functional theory (DFT) with the basis set 6-311++G (d, p). The frontier molecular orbital (FMO) energies, absorption wavelengths, and electronic characteristics (total energy and energy range) of the 2BA were calculated using the B3LYP and M06-2X levels of time-dependent DFT (TD-DFT) with the 6-311++G (d, p) basis set. The TD-DFT method, employing the integral equation formalism-polarized continuum model (IEF-PCM), was utilized to investigate electronic transitions within the solvent environment (ethanol and methanol). When calculations performed using two different methods were compared with experimental values, the results closest to the experimental values were obtained using the TD-DFT/B3LYP method in ethanol. Photovoltaic parameters such as light harvesting efficiency (LHE), open-circuit voltage (V_{oc}), driving force for electron injection (ΔG_{inj}), and driving force for dye regeneration (ΔG_{reg}) were similarly calculated and analyzed. LHE calculations showed that the DFT/M06-2X method calculated better values than the TD-DFT/B3LYP method.

Keywords: *DFT, energy, photovoltaic*

1. Introduction

The environmental impacts of fossil fuels and rising energy demand have led researchers to pursue clean and renewable energy sources. In this context, Dye-Sensitized Solar Cells (DSSC), due to their low production costs and flexible structures, are a strong alternative to silicon-based photovoltaic systems [1]. The efficiency of DSSCs largely depends on the dye molecules (sensitizers) that adhere to the semiconductor surface (typically) and absorb sunlight [1, 2]. The photovoltaic potential of this molecule stems from both its optical behavior within metal complexes and the carboxylic acid groups that enable it to attach to semiconductor surfaces [1, 3]. 2,2'-Biquinoline-4,4'-dicarboxylic acid (2BA) is an important organic ligand in this field. It is an important organic molecule. Due to its strong photoluminescence and electroluminescence properties, it finds applications not only in solar cells but also in light-emitting devices and electro-optic displays [3-6].

Another factor affecting the photovoltaic performance of the 2BA is its interaction with the semiconductor surface. Wojtal and Zhitomirsky used the 2BA in surface modification of inorganic particles and electrophoretic deposition processes to ensure stable film formation [3]. Bae et al., on the other hand, investigated electron transfer rates on the surface of ruthenium-biquinoline complexes and emphasized the effects of the hydrophobic character of the ligand structure on its stability during this process [2].This broad perspective shows that the 2BA is not merely a dye but also a versatile building block for complex photovoltaic and optoelectronic systems.

Fluorescence emissions of 2BA-based complexes are critically important for understanding photovoltaic processes. Shankar and Baruah investigated how stacking effects modulate fluorescence emission in Cu complexes [5]. Additionally, the gas transport and electrochemical properties of polymeric structures containing biquinoline units (polybenzoxazinoneimides) have been studied, and their stable redox behavior when complexed with ruthenium has been reported [7, 8].

This study investigates the electronic and photovoltaic properties of the 2BA in different environments (gas phase, ethanol, and methanol). Calculations were performed using the DFT method and two different hybrid functionals, B3LYP and M06-2X. Its potential

*Corresponding author: hatice.vural@amasya.edu.tr

as a dye material for dye-sensitized solar cells was also investigated.

2. Computational Details

All calculations were performed using the GAUSSIAN 09W program [9] and visualized using the GaussView05 program [10]. The DFT and TD-DFT methods B3LYP [11] and M06-2X [12] hybrid functional with 6-311++G (d, p) basis set were used to calculate electronic and photovoltaic parameters. The Highest Occupied Molecular Orbital (HOMO), Lowest Unoccupied Molecular Orbital (LUMO), energy gap (ΔE), chemical hardness (*η)*, chemical potential (μ), softness (*s*), and electronegativity (χ) of the 2BA were calculated using the same levels in the gas phase, ethanol, and methanol.

By using the Frontier Molecular Orbitals (FMOs) [HOMO and LUMO] energy values of the 2BA obtained at DFT method, ionization potential [I = -E_{HOMO}], electron affinity [A = -E_{LUMO}] energy gap (ΔE), chemical hardness (*η)*, chemical potential (μ), softness (*s*), and electronegativity (χ), which are global chemical reactivity parameters, were obtained using Equations (1)-(5) [13-15].

$$\Delta E = E_{LUMO} - E_{HOMO} \quad (1)$$

$$\eta = \frac{(E_{LUMO} - E_{HOMO})}{2} \quad (2)$$

$$\mu = \frac{(E_{HOMO} + E_{LUMO})}{2} \quad (3)$$

$$\chi = -\mu \quad (4)$$

$$S = \frac{1}{2\eta} \quad (5)$$

3. Result and Discussion

3.1. Frontier Molecular Orbitals and Reactivity Descriptors

The optimized geometry of the 2BA [16] was performed using the DFT method B3LYP and M06-2X functional with 6-311++G (d, p) basis set. The optimized structures of the 2BA are shown in Figure 1.

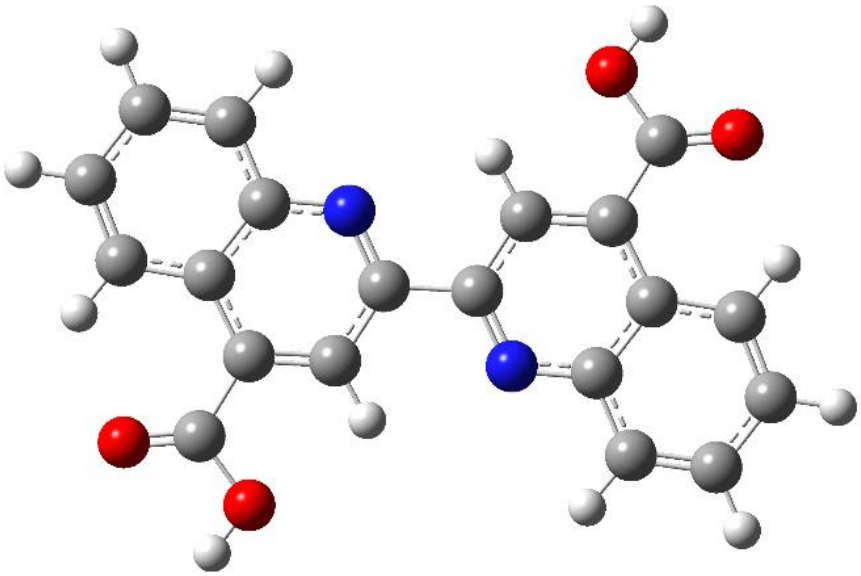

Figure 1. The geometric structure of 2BA was optimized using the DFT/B3LYP method.

The FMO energies, energy gaps, and global reactivity parameters derived from TD-DFT simulations produced varying findings for two distinct functionals of the 2BA in both the gas phase and in ethanol and methanol environments.

The ΔE value of the 2BA was calculated to be greater when employing the TD-DFT/M06-2X method compared to the TD-DFT/B3LYP method. Calculations of the energy gap for 2BA utilizing the M06-2X and B3LYP levels yielded comparable results between gas phase and solvent phase analyses. This value was calculated as 3.83 eV in the gas phase, 3.82 eV in ethanol, and 3.82 eV in methanol using the TD-DFT/B3LYP method, while it was calculated as 6.03 eV in the gas phase, 6.01 eV in ethanol, and 6.01 eV in methanol using the TD-DFT/ M06-2X method.

Table 1. The FMO energies and related properties for 2BA

TD-DFT	Gas phase		Ethanol		Methanol	
Parameters	**M06-2X**	**B3LYP**	**M06-2X**	**B3LYP**	**M06-2X**	**B3LYP**
E_{HOMO} **(eV)**	-7.85	-6.65	-7.98	-6.73	-7.98	-6.73
E_{LUMO} **(eV)**	-1.82	-2.82	-1.97	-2.91	-1.97	-2.91
ΔE **(eV)**	6.03	3.83	6.01	3.82	6.01	3.82
I **(eV)**	7.85	6.65	7.98	6.73	7.98	6.73
A **(eV)**	1.82	2.82	1.97	2.91	1.97	2.91
χ **(eV)**	4.83	4.73	4.97	4.48	4.97	4.48
η **(eV)**	3.01	1.91	3.00	1.91	3.00	1.91
μ **(eV)**	-4.83	-4.73	-4.97	-4.48	-4.97	-4.48
s **(eV^{-1})**	0.16	0.26	0.17	0.26	0.17	0.26

The η, χ, and μ parameters of the 2BA in the gas phase were calculated as 1.91, 4.73, and -4.73 eV, respectively, using the B3LYP level. In ethanol, these parameters were calculated as 1.91, 4.48, and -4.48 eV, respectively, using the B3LYP method. The same parameters were calculated as 3.01, 4.83, and -4.83 eV in the gas phase, respectively, using the TD-DFT/M06-2X method, while they were calculated as 3.0, 4.97, and -4.97 eV in ethanol, respectively. The η values obtained using the M06-2X level imply that the molecule may exhibit low reactivity and resistance to load deformation, but the B3LYP level indicates that 2BA has a diminished hardness value and may have significant chemical reactivity.

3.2. Optical Analysis

The experimental spectrum of the 2BA exhibits three absorption bands at 208 nm, 260 nm, and 332 nm [17]. The electronic absorption spectra and transitions of the 2BA in both gas phase and solvent (ethanol and methanol) were computed utilizing the TD-DFT method with M06-2X and B3LYP hybrid functionals, employing the 6-311++G (d, p) basis set. The solvent effect was assessed using IEF-PCM. Table 2 lists the UV-vis spectrum data of the 2BA using the GaussSum software [18], which was produced using two different methods and different media. Figures 2 and 3 show the UV-Vis absorption spectra calculated for 2BA using two different methods.

When comparing the UV-Vis absorption spectrum data obtained from the TD-DFT/B3LYP simulation of the 2BA with experimental data, it is observed that the calculations performed using the solvent are in very good agreement with the experimental value. Comparison of the UV-Vis absorption spectrum data derived from the TD-DFT/M06-2X simulation of the 2BA with experimental data revealed that the gas phase calculations exhibited superior concordance with the experimental values. The computations in the solvent medium resulted in a little reduction in wavelength.

The largest absorption peak of 2BA, calculated using the TD-DFT/B3LYP method, was found to be 356 nm in the gas phase and 362 nm in ethanol and methanol. This band was found to be 362 nm in the gas phase and 305 nm in ethanol and methanol using the TD-DFT/ M06-2X method. According to TD-DFT/B3LYP results, the longest absorption band corresponds to the electronic transition calculated as HOMO→LUMO (87%) in the gas phase, HOMO→LUMO (91%) in ethanol, and HOMO→LUMO+1 (91%) in methanol (Fig.4). These transitions were calculated using the TD-DFT/ M06-2X method as HOMO→LUMO (91%) in the gas phase, HOMO→LUMO+1 (81%) in ethanol, and HOMO→LUMO+1 (81%) in methanol (Fig.5). When calculations performed using two different methods are compared with experimental values, it can be said that the closest results to experimental values were obtained using the TD-DFT/B3LYP method and the ethanol solution.

For 2BA, using the TD-DFT/B3LYP method, it was predicted that the bands calculated in the gas phase in the range of 325-260 nm, and in ethanol and methanol in the range of 338-263 nm, are n→π* and π→π* transitions. According to the TD-DFT/ M06-2X method results, these transitions were calculated to be in the range of 338-263 nm in the gas phase and 254-232 nm in ethanol and methanol.

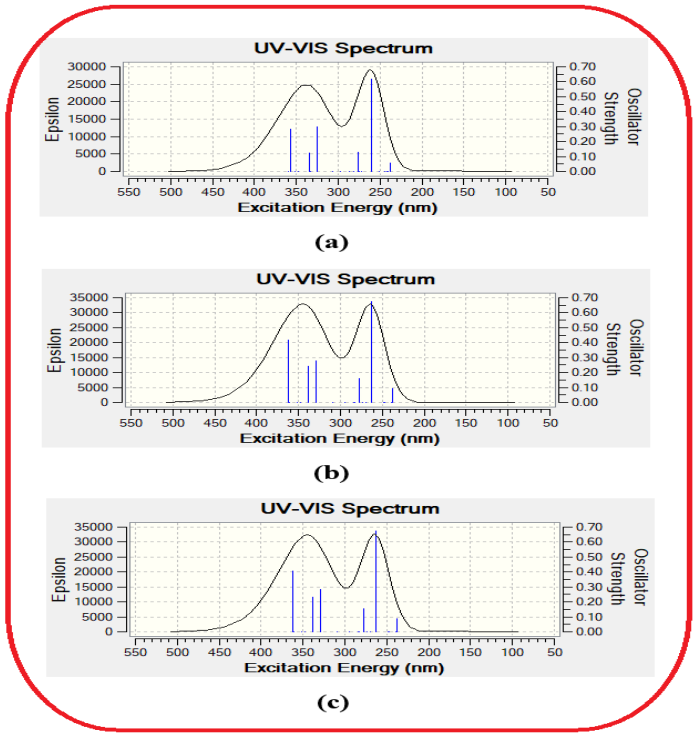

Figure 2. UV-Vis absorption spectra of 2BA obtained by TD-DFT/B3LYP simulation are shown in (a) gas phase, (b) ethanol, and (c) methanol.

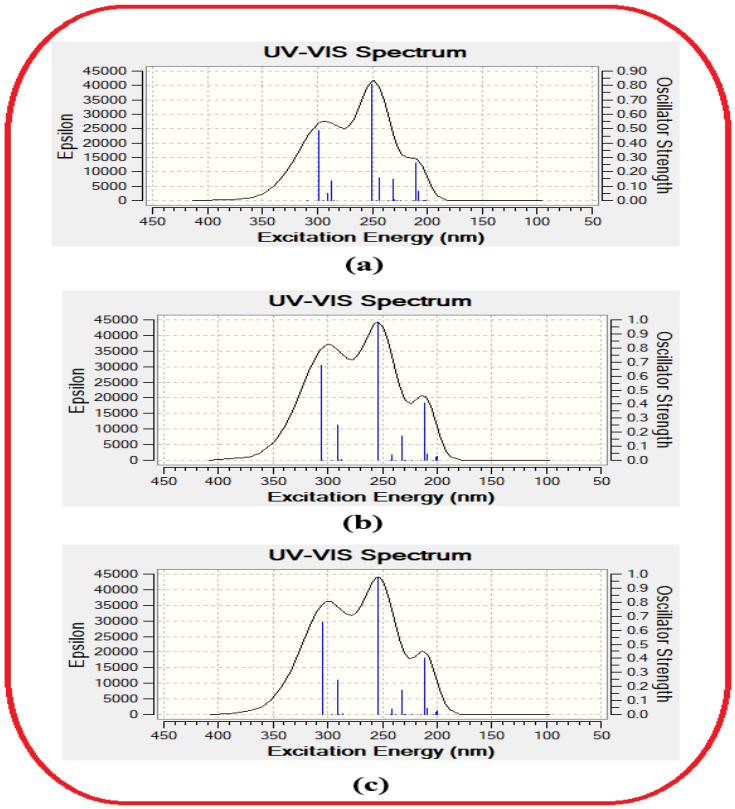

Figure 3. UV-Vis absorption spectra of 2BA obtained by TD-DFT/M06-2X simulation are shown in (a) gas phase, (b) ethanol, and (c) methanol.

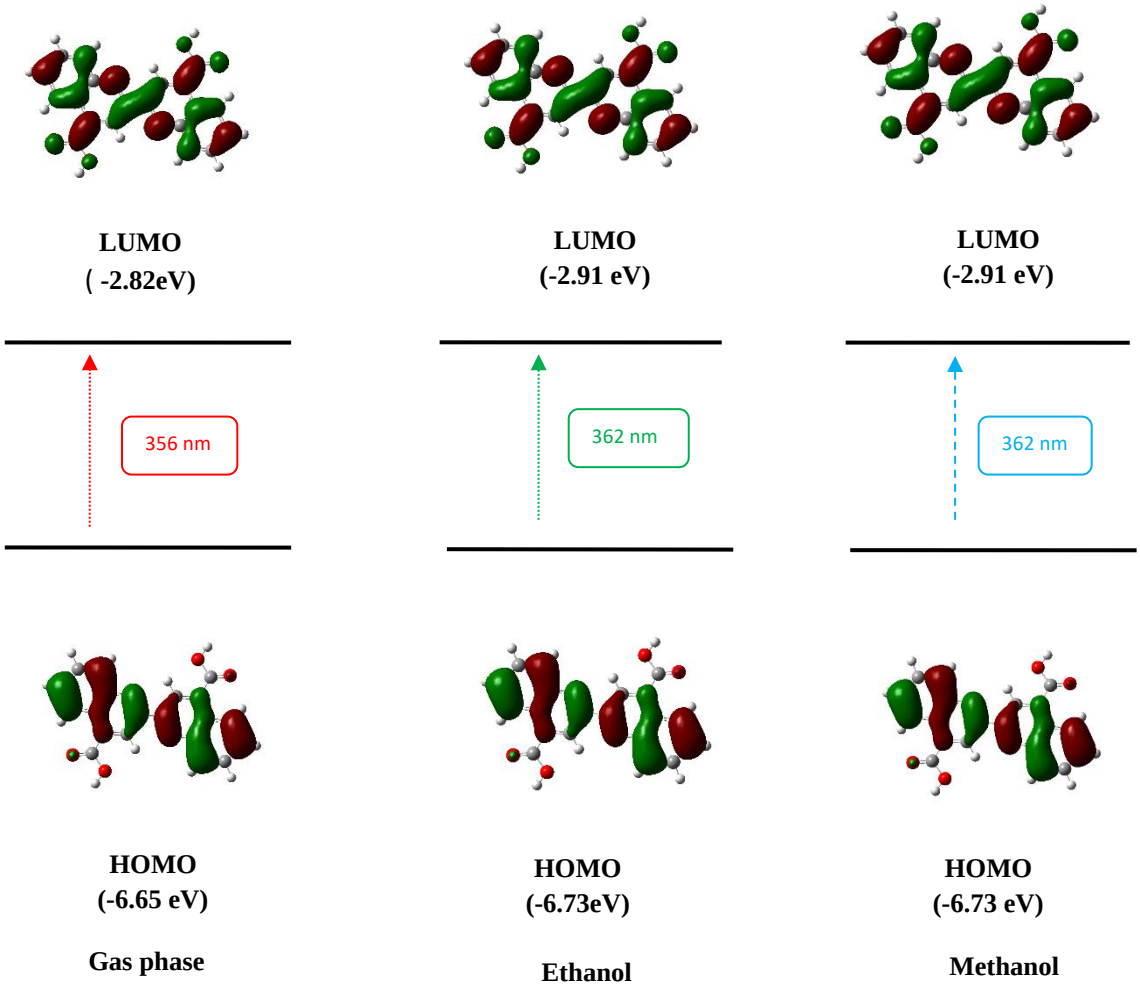

Figure 4. Frontier molecular orbitals of the 2BA calculated using the TD-DFT/B3LYP method.

Table 2. Calculated electronic transitions for 2BA with the TD-DFT/ IEF-PCM method.

TD-DFT	Solvent	λ (nm)	E (eV)	Osc. Strength(f)	Major Contributions
B3LYP	Gas	356	**3.48**	0.285	H → L (+87%)
		325		0.300	H-1→ L+1 (+87%)
		260		0.615	H-4→ L+1 (+32%)
	Ethanol	362	**3.42**	0.419	H → L (+91%)
		338		0.240	H-2→ L (+94%)
		263		0.676	H-4→ L+1 (+36%)
	Methanol	362	**3.42**	0.407	H → L (+91%)
		338		0.232	H-2→ L (+94%)
		263		0.672	H-4→ L+1 (+35%)
M06-2X	Gas	362	**3.42**	0.407	H→L (+ 91%)
		338		0.232	H-2 → L (+94%)
		263		0.672	H-4→ L+1 (+35%)
	Ethanol	305	**4.06**	0.674	H → L (+81%)
		254		0.983	H-1→ L+1 (+54%)
		232		0.173	H-3→ L+1 (+14%)
	Methanol	305	**4.06**	0.657	H → L (+81%)
		254		0.978	H-1→ L+1 (+54%)
		232		0.170	H-3→ L+1 (+14%)

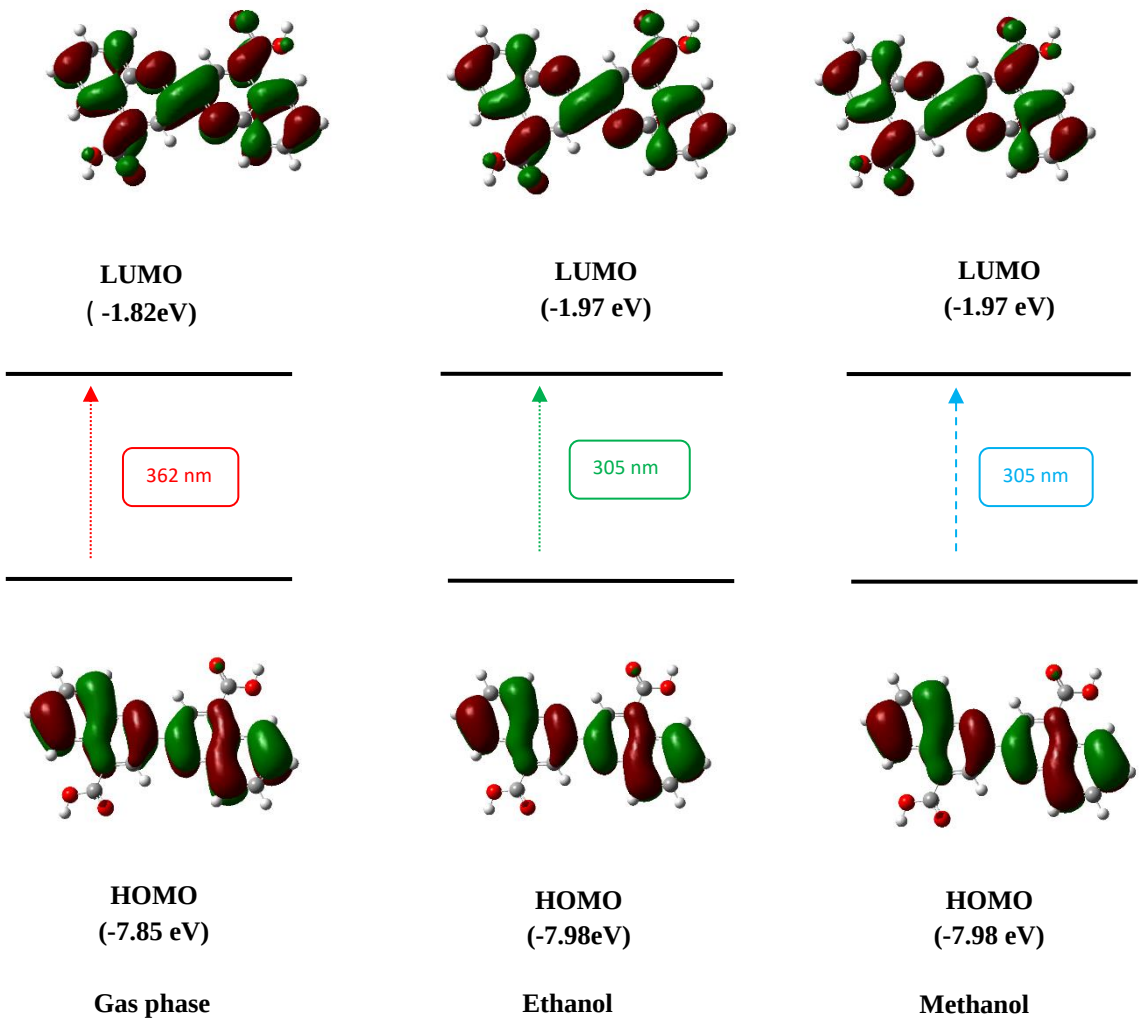

Figure 5. Frontier molecular orbitals of the 2BA calculated using the TD-DFT/M06-2X method.

3.3. Photovoltaic Performance

Photovoltaic factors include *LHE* (Light Harvesting Efficiency), open voltage (V_{oc}), the driving force for electron injection (ΔG_{inj}), and the driving force for regeneration of dye (ΔG_{reg}), which are important for creating efficient DSSCs (Eq. 6-9). We have calculated the parameters as follows [19-22]:

$$V_{OC} = E_{LUMO} - E_{CB} \quad (6)$$

$$LHE = 1\text{-}10^{-f} \quad (7)$$

$$\Delta G_{inj} = E^{dye*} - E_{CB} \quad (8)$$

$$\Delta G_{reg} = E^{dye} - E_{red}^{Elect} \quad (9)$$

where f is the title complex's oscillator strength corresponding to the λ_{max} wavelength, E^{dye*} is excited state oxidation potential energy of the complex, E_{CB} is the conduction band of the TiO_2 (-4.00 eV), E^{dye} is oxidation potential energy of the complex at the ground state, E_{red}^{Elect} is the redox potential energy of the electrolyte (-4.85 eV) [23].

The LHE, V_{oc}, ΔG_{inj}, and ΔG_{reg} parameters of the 2BA were computed using two different functionals with the TD-DFT method and in different environments and are given in Table 3. A system must possess a greater open circuit voltage-current to efficiently capture light [24-26]. The V_{oc} value of the complex was calculated as 1.18 eV in the gas phase and 1.09 eV in ethanol and methanol using the DFT/B3LYP method. This parameter was obtained as 2.18 eV in the gas phase and 2.03 eV in ethanol and methanol using the DFT/M06-2X method. Comparing the results obtained from the two different methods, it is observed that the DFT/M06-2X method results are higher. Furthermore, in both methods, the results

obtained in the gas phase are greater than those obtained in the solvent environment.

Calculating the LHE value for 2BA using the DFT/B3LYP method yielded higher calculation results in the solvent medium compared to the gas phase, while the DFT/M06-2X method resulted in higher values in the gas phase compared to the solvent. According to Table 3, negative ΔG_{inj} values were obtained in all media in the B3LYP results (-0.83 and -0.69 eV), while in the M06-2X results, a positive value (+0.43 eV) was found in the gas phase, and the values became slightly negative in the solvent medium (-0.08 eV). Therefore, it can be said that the DFT/B3LYP method will show a more suitable injection behavior in terms of DSSC.

All media had negative ΔG_{reg} values. This indicates that the oxidized dye can be easily reduced by the electrolyte. The M06-2X method revealed much more substantial negative results (-3.13 eV), suggesting that regeneration may occur considerably.

Table 3. Calculated photovoltaic parameters for 2BA with the TD-DFT/ IEF-PCM method.

TD-DFT	**Gas phase**		**Ethanol**		**Methanol**	
Parameters	**M06-2X**	**B3LYP**	**M06-2X**	**B3LYP**	**M06-2X**	**B3LYP**
E_{HOMO} **(eV)**	-7.85	-6.65	-7.98	-6.73	-7.98	-6.73
E_{LUMO} **(eV)**	-1.82	-2.82	-1.97	-2.91	-1.97	-2.91
ΔE **(eV)**	6.03	3.83	6.01	3.82	6.01	3.82
LHE	0.61	0.48	0.79	0.61	0.78	0.61
V_{OC}	2.18	1.18	2.03	1.09	2.03	1.09
E_{ox}^{dye*}	4.43	3.17	3.92	3.31	3.92	3.31
ΔG_{inj}	0.43	-0.83	-0.08	-0.69	-0.08	-0.69
ΔG_{reg}	-3	-1.8	-3.13	-1.88	-3.13	-1.88

4. Conclusions

In this study, the electronic and photovoltaic parameters of the 2BA were investigated using the B3LYP and M06-2X hybrid functionals and the 6-311++G (d, p) basis set of the DFT method. According to UV-Vis absorption spectral data, the results most consistent with the experimental values of 2BA were obtained from calculations performed with DFT/B3LYP and in the solvent phase, and from calculations performed with DFT/ M06-2X in the gas phase. The ΔE calculations for 2BA show that the value obtained using the TD-DFT/M06-2X method is higher than that obtained using the TD-DFT/B3LYP method. The highest V_{oc} value for 2BA was derived from calculations conducted using the TD-DFT/M06-2X technique in the gas phase. The maximum LHE value for 2BA was obtained by calculations performed using the TD-DFT/M06-2X method in a solvent phase. This study is expected to contribute to future research on high-performance dye-sensitized solar cells.

Acknowledgment

This work was supported by Amasya University Research Fund for financial support through Project number FMB-BAP 25-0635. The authors thank the Amasya University Scientific Research Projects Unit for financial support.

References

[1]. Wills, K. A., Mandujano-Ramírez, H. J., Merino, G., Mattia, D., Hewat, T., Robertson, N. & Cameron, P. J. (2013). Investigation of a copper (I) biquinoline complex for application in dye-sensitized solar cells. *RSC advances*, *3*(45), 23361-23369.

[2]. Bae, J. H., Kim, D., Kim, Y. I., & Kim, K. (1996). *Photoinduced Electron Transfer from Ru(II) to TiO2 Complexes at Nanocrystalline TiO2 Electrodes*.

[3]. Wojtal, P., & Zhitomirsky, I. (2016). Surface modification and electrophoretic deposition of materials using 2, 2′-biquinoline-4, 4′-dicarboxylic acid. *Materials Letters*, *174*, 44-47.

[4]. Dai, P.-X., Yang, E.-C., Wang, X.-G., & Zhao, X.-J. (2008). *Synthesis, Crystal Structures and Fluorescent Properties of Two 2,2-Biquinoline-4,4-dicarboxylate-based Cadmium(II) and Cobalt(II) Complexes*.

[5]. Shankar, K., & Baruah, J. B. (2016). Modulation of Fluorescence Emissions of Copper(II) 2,2′-biquinoline-4,4′-dicarboxylates. ChemistrySelect, 1(12), 3038–3044.

[6]. Xie, J. (2009). Twodimensional Metal-Organic Framework [Zn(bqdc)]n (bqdc = 2,2′-biquinoline-4,4′-dicarboxylate) – Synthesis, Crystal Structure and

Spectral Characterization. Zeitschrift Für Anorganische Und Allgemeine Chemie, 635(2), 384–388.

[7]. Goikhman, M. Ya., Podeshvo, I. V., Magdesieva, T. V., Nikitin, O. M., Butin, K. P., Yakimanskii, A. V., & Kudryavtsev, V. V. (2006). Synthesis and Electrochemical Properties of Ruthenium(II) Complexes with Biquinoline-Containing Polyamic Acids— Polybenzoxazinone Prepolymers.

[8]. Polotskaya, G. A., Guliy, N., Goĭkhman, M. Ya., Podeshvo, I. V., Brožová, L., & Pientka, Z. (2015). Structure and Gas Transport Properties of Polybenzoxazinoneimides with Biquinoline Units in the Backbone. Macromolecular Symposia, 348(1), 44–53.

[9]. Gaussian 09, Revision A.1, M.J. Frisch, G.W. Trucks, H.B. Schlegel, G.E. Scuseria, M.A. Robb, J.R. Cheeseman, G. Scalmani, V. Barone, B. Mennucci, G.A. Petersson, H. Nakatsuji, M. Caricato, X. Li, H.P. Hratchian, A.F. Izmaylov, J. Bloino, G. Zheng, J.L. Sonnenberg, M. Hada, M. Ehara, K. Toyota, R. Fukuda, J. Hasegawa, M. Ishida, T. Nakajima, Y. Honda, O. Kitao, H. Nakai, T. Vreven, J.A. Montgomery, Jr., J.E. Peralta, F. Ogliaro, M. Bearpark, J.J. Heyd, E. Brothers, K.N. Kudin, V.N. Staroverov, R. Kobayashi, J. Normand, K. Raghavachari, A. Rendell, J.C. Burant, S.S. Iyengar, J. Tomasi, M. Cossi, N. Rega, J.M. Millam, M. Klene, J.E. Knox, J.B. Cross, V. Bakken, C. Adamo, J. Jaramillo, R. Gomperts, R.E. Stratmann, O. Yazyev, A.J. Austin, R. Cammi, C. Pomelli, J.W. Ochterski, R.L. Martin, K. Morokuma, V.G. Zakrzewski, G.A. Voth, P. Salvador, J.J. Dannenberg, S. Dapprich, A.D. Daniels, O. Farkas, J.B. Foresman, J.V. Ortiz, J. Cioslowski, D.J. Fox, Gaussian, Inc., Wallingford CT, 2009.

[10]. GaussView, Version 5, Roy Dennington, Todd Keith and John Millam, *Semichem Inc.*, Shawnee Mission KS, 2009.

[11]. Lee, C., Yang, W, Parr, R.G., *Phys. Rev.* B37 (1988), 785-789.

[12]. Zhao, Y., & Truhlar, D. G. (2008). The M06 suite of density functionals for main group thermochemistry, thermochemical kinetics, noncovalent interactions, excited states, and transition elements: two new functionals and systematic testing of four M06-class functionals and 12 other functionals. *Theoretical chemistry accounts*, *120*(1), 215-241.

[13]. Yang, W. and Parr, R. G. (1985). Hardness, Softness, and the Fukui Function in the Electronic Theory of Metals and Catalysis. *Proceedings of the National Academy of Sciences of the United States of America*, 82, 6723–6726.

[14]. Chattaraj, P. K., Sarkar, U. and Ro, D. R. (2006). Electrophilicity Index. *Chemical Reviews* 106, no. 6, 2065–2091.

[15]. İşler, E., Zülfikaroğlu, A., Vural, H., & Dege, N. (2022). Synthesis, spectroscopic analyses, DFT calculations and molecular docking studies of Pd (II) complex of hydrazone ligand derived from ethyl carbazate. *Molecular Crystals and Liquid Crystals*, *736*(1), 72-92.

[16]. Zhang, J. X., & Halling, P. J. (1990). pH and buffering in the bicinchoninic acid (4, 4′-dicarboxy-2, 2′-biquinoline) protein assay. *Analytical biochemistry*,*188*(1), 9-10.

[17]. Wojtal, P., & Zhitomirsky, I. (2016). Surface modification and electrophoretic deposition of materials using 2, 2′-biquinoline-4, 4′-dicarboxylic acid. *Materials Letters*, *174*, 44-47.

[18]. O'boyle, N. M., Tenderholt, A. L., & Langner, K. M. (2008). Cclib: a library for package-independent computational chemistry algorithms. *Journal of computational chemistry*, *29*(5), 839-845.

[19]. Hagfeldt, A. and Vlachpoulos, N. (2018). Dye-sensitized solar cells, in: The Future of Semiconductor Oxides in Next-Generation Solar Cells, Elsevier, pp. 183-239.

[20]. Hassan, A. U., Sumrra, S. H., Zubair, M., Mustafa, G., Noreen, S., & Imran, M. (2023). Correlating the charge density and structural fabrication of new organic dyes to create visible light harvesting materials with tunable NLO refining: insights from DFT. *Chemical Papers*, *77*(10), 6183-6202.

[21]. Adeloye, A. O., Koudjina, S., Kumar, V., Tapala, K. C., Gbenou, J. D., & Chetti, P. (2025). One-pot synthesis, photophysical, electrochemical and molecular property of mixed-ligands ruthenium complex functionalities: Potential materials for dye-sensitized solar cells (DSSCs). *Dyes and Pigments*, *235*, 112626.

[22]. Rajpurohit, A. S., Benedict, A., Kathiravan, A., Ashish, A., & Jaccob, M. (2026). Exploring the influence of amine donors on the photophysical properties of thiazolidine linked cyanoacrylic acid dyes: A theoretical study. *Spectrochimica Acta Part A: Molecular and Biomolecular Spectroscopy*, 127691.

[23]. Fatima, K., Manzoor, T., Nazir, I., Ganaie, F. A., Qureashi, A., Bashir, A., & Pandith, A. H. (2024). Unveiling the molecular symphony-A DFT exploration of structure, electronic dynamics, and excited state electron transfer in D-π-A systems, enhanced by TeO2@ GQD multi-junctions for solar energy conversion in DSSC. *Solar Energy Materials and Solar Cells*, *273*, 112964.

[24]. Dhuliya, V., Purohit, L. P., Lakhera, S., & Rana, M. (2025). Potentiality of 1-(4-nitrophenyl)-2-pyrrolidine methanol as an efficient photosensitizing material: A multi-solvent first principle DFT study. *Materials Science in Semiconductor Processing*, *188*, 109231.

[25]. Nagaveni, K., Hegde, M. S., Ravishankar, N., Subbanna, G. N., & Madras, G. (2004). Synthesis and structure of nanocrystalline TiO2 with lower band gap showing high photocatalytic activity. *Langmuir*, *20*(7), 2900-2907.

[26]. Lakhera, S., Devlal, K., & Rana, M. (2023). Nonlinear optical response of silver trimer adsorbed para-aminobenzoic acid: a DFT study. *Physica Scripta*, *98*(11), 115519.